

# ULTRASOUND LOCALIZATION MICROSCOPY OF THE BRAIN: THE MISSING MICRO VASCULATURE

Stephen A. Lee<sup>1</sup>, Jonathan Porée<sup>1</sup>, Alexis Leconte<sup>1</sup>, Alice Wu<sup>1</sup>, Jean Provost<sup>1,2</sup>

<sup>1</sup>Department of Engineering Physics, Polytechnique Montreal, Montreal, Canada.

<sup>2</sup>Montreal Heart Institute, Montreal, Canada.

## ABSTRACT

Ultrasound Localization Microscopy (ULM) is a powerful technique able to realize the brain microvasculature down to the micron level. Despite recent developments into retrieving more functional information (i.e., pulsatility measurements, blood flow velocity, and neurovascular coupling), there is still a need for biomarkers with high clinical significance. Capillaries, the microvascular unit at the interface between neurons and the circulatory system, may be important biomarkers for neural health. However, ULM in its current iteration cannot readily, with confidence, proclaim to capture capillary dynamics. Thus, this paper aims to explore the question, where are capillaries in ULM? We propose a solution involving long ensemble lengths for input into spatiotemporal singular value decomposition clutter filters to recover velocity profiles that exhibit capillary flow behavior. We show that with longer ensembles, we can retrieve more capillary units than standard implementations.

**Index Terms**— Ultrasound Localization Microscopy, SVD, capillary, dynamic, biomarkers

## 1. INTRODUCTION

The adaptation of optical super resolution approaches to ultrasound imaging created Ultrasound Localization Microscopy (ULM) [1]. Via the introduction of micron-sized microbubble contrast agents to the vasculature, we can capture high frame-rate ultrasound images of the brain through the skull, selectively filter out slow-moving tissue via a singular value decomposition (SVD)-based clutter filter [2], localize the centers of these bubble point-spread function (PSF), and follow their trajectory over time. In reconstructing and accumulating these tracks, we attain images of the brain microvasculature and their velocity profiles at depth with spatial resolutions breaking the diffraction limit of conventional ultrasound.

However, to garner support for clinical adoption of such a methodology, functional information regarding brain health should be of the utmost priority. In pursuit of such endeavors, ULM can be temporally realigned to visualize the dynamic movement of these bubbles and measure relative

pulsatility – so called dynamic ULM (dULM) [3]. Despite these advances towards functional ULM, an important microvascular unit seems to be missing in ULM – the capillaries that connect the input arterial networks to the output venous networks [4]. It is here at this junction, that oxygenated blood cells transfer their nutrients to the surrounding neurons. It has been hypothesized that in neurological disease and disorder that exhibit symptoms in the vasculature, dysfunction will occur in capillaries first [5]. Thus, one could imagine the importance of imaging and measuring the functionality of these microvascular units in monitoring disease progression and early detection. Thus, we ask the question, “where are the capillaries in ULM?”

### 2.1. It’s a matter of motion

ULM is a technique based on the differentiation between regimes of motion – scatterers from blood will move at velocities faster than the surrounding stationary tissue [6]. In

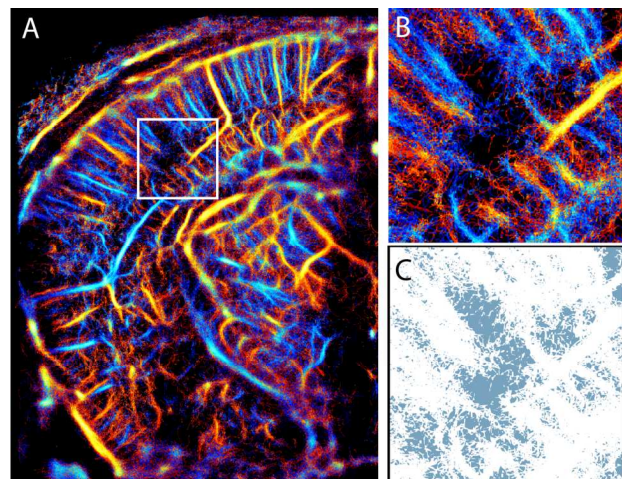


**Fig. 1.** ULM image of the mouse brain. (A) one hemisphere with directional color maps indicating upwards and downwards flow. (B) Zoom up of the ROI in (A). (C) negative image highlighting the space in between larger vessels where capillaries should be.

the context without microbubble contrast agents, power Doppler summation of large ensembles of ultrasound frames after SVD clutter filtering will reveal diffraction limited images of the blood. When microbubbles are introduced to the vascular, the same operation can reveal distinct PSFs that can then have their centers localized and tracked over time for ULM (Fig. 1A).

The SVD clutter filter operation decomposes a spatiotemporal composition of the data into eigenspaces (i.e., skull and brain tissue) and removal of singular values leaves more decorrelated signals remaining (i.e., blood and noise) [2]. The cutoff between blood signal and stationary tissue is often overlapped and becomes tougher to distinguish in situations with large motion artifacts, due to breathing or pulsation. Thus, in practice, the eigenvalue threshold is usually set sufficiently high as to remove the majority of stationary tissue. The unintended result of this, however, is the removal of microbubbles moving at very low velocities, and thus, the space surrounding larger penetrating arterials and veins where capillaries should be are dark.

We know from optical microscopy that capillaries occupy the space in between the large vessels as their ability to supply neurons with nutrients is positively impacted by surface area. Importantly, the blood flow velocity in these small vessels is much slower than the penetrating arteries and veins. Herein lies the problem, ULM, at its core with intense simplification, is very much a movement-based imaging technique that discriminates fast blood signal from stationary and slow-moving brain tissue to map the microvasculature. What happens when a slow-moving microbubble moves into a capillary when its speed is on par with the surrounding tissue movement?

## 2.2. It's a matter of time

Given that blood moving through capillaries operate at velocities often on the same order of magnitude as tissue, a clutter-filter, based on removal of slow-moving singular values, would also remove these signals. Fig. 2 shows the power spectral density for in-phase/quadrature (IQ) data (ensemble length 600) as a function of increasing singular values where the singular values correspond to tissue, blood and noise. In a sense, the ensemble length in time directly affects the sampling in frequency space. Lastly, the slow blood flow velocity in the capillaries means that bubbles perfusing capillaries are sparse and can take upwards of 10 seconds, necessitating the use of longer imaging sequences to capture the whole trajectory behavior and velocity profiles. Thus, we hypothesize that increasing the ensemble length of our acquisitions (i.e., 600 to 6000 frames), can more easily discriminate the separation of tissue signal (i.e., brain and skull) from slow moving bubbles traversing capillary networks, ultimately recovering more tracks corresponding to capillaries.

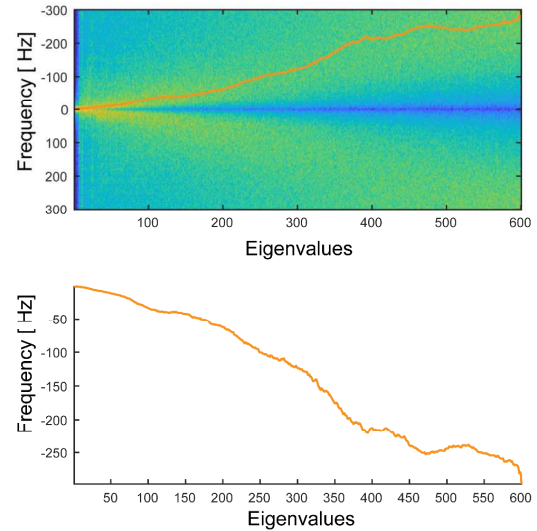


**Fig. 2.** Power spectral density as a function of eigenvalues. (Top) negative and positive frequencies calculated for right singular values. (Bottom) mean frequency curve with horizontal lines at expected regime changes.

## 3. MATERIALS & METHODS

### 3.1. Animals

All experiments were performed in accordance with the Animal Research Ethics Committee of the Montreal Heart Institute (Protocol # 2023-32-02 TAC-ultrasounds). Female C57BL/6J mice (Envigo, IN, USA) ages 8 to 10 weeks were used in all experiments and kept to an absolute minimum. Animals were anesthetized with isoflurane (2% -1L O<sub>2</sub> for induction; 1-1.5% - 0.5-1L O<sub>2</sub> for management). Preparation for microbubble injection was performed using a catheter tail-vein injection via 27G needles. Physiological saline was used to test vessel patency and confirmation of tail-vein placement. During the imaging experiment, a bolus injection of 4  $\mu$ L per g of body weight Definity microbubbles (Lantheus, MA, USA), diluted in physiological saline at a 1:10 ratio, was injected through the catheter.

### 3.3 Ultrasound Imaging Parameters

ULM was performed using a linear hockey-stick array with a center frequency of 10 MHz and a bandwidth between 8 and 18 MHz (L8-18ID, GE, IL, USA) and interfaced with a Vantage research ultrasound machine (Verasonics, WA, USA) to acquire IQ data (100% bandwidth sampling). Ultrasound image stacks of 600 frames were acquired using 7 tilted plane waves at angles between -11° and 11° at a compounded pulse repetition frequency (PRF) of 900 Hz for a total of 4500 Hz total frame rate. To increase transcranial microbubble signal, harmonic imaging was performed by transmitting plane waves at 7.8125 MHz and received at 15.625 MHz. IQ data was then beamformed using a

conventional GPU-based delay and sum algorithm onto a grid with a spacing of  $\lambda/3$ .

### 3.4 Experimental design and long-ensemble SVD

Ultrasound stacks were acquired in a continuous manner where data is being off-loaded from memory at a sustainable rate for acquiring the next ultrasound stack. This allowed us to compare three conditions: (1) short-ensemble (SE-SVD; ensemble length 600: 0.6 s), (2) multi-short-ensemble (MSE-SVD; ensemble length 600 x 10: 6 s), and (3) long-ensemble (LE-SVD; ensemble length 6000: 6s).

### 3.4 SVD temporal frequency analysis

Analysis of the contribution of eigenvalue from SVD on the temporal frequency is based on methods from [2]. Briefly, stacks of IQ data were transformed into a spatiotemporal casorati matrix representation where the SVD is operated on the covariance. A periodogram with a 0.2 Tukey window is then operated on the right singular matrix. A moving average of the mean frequency response for one side of the periodogram is then calculated for further analysis.

### 3.5 Ultrasound Localization Microscopy Analysis

SVD-filtered data can then be tracked and localized via a spatiotemporal process [7]. Before super resolution tracking, IQ data is filtered via a Hessian-based vesselness filter that operates over space and time, specifically-tuned to the expected PSF of a microbubble. Subpixel localization is performed with *a priori* knowledge of the centers of the bubble (given by the centerline) and updated via radial symmetry with *a posteriori* information given by the IQ data.

Tracks are then Kalman filtered, spline interpolated, and derivate to produce estimates of the velocity.

### 3.5 Capillary analysis

To classify capillary trajectories, we measure the symmetry in the track (indicating the entrance and exit of a bubble through a capillary), we fit two exponentials to the beginning and ends of the trajectories. The  $R^2$  value was used to assess the likelihood that the track corresponds to a capillary. These tracks were split into full capillary tracks, starts, and ends, where the starts are characterized by an exponential decrease in the velocity and the opposite for the ends. From simulations of the brain microvasculature [9], we can imagine the different travel paths of a microbubble. Bubbles that are in penetrating veins and arteries, regardless of in and out of imaging plane travel, will have relatively constant velocity throughout their travel. Bubbles that enter capillaries will have to slow down and speed up when they exit these meshes. Additionally, we assume that capillaries will not have large travel distances since their function is to provide nutrients to the surrounding perfused brain tissue

## 4. RESULTS

### 4.1 Increasing ensemble length increases frequency discrimination

Fig 3. illustrates the results of LE-SVD. Here, we see most of the spectral density is concentrated below the first 1000 eigenvalues. The mean spectral frequency below the first 1000 eigenvalues does not exhibit inflection points as shown in Fig 2, rather, the spectral density linearly increases with eigenvalues. Thus, we expect that with the same eigenvalue cutoff values, we can recover slower microbubble signals.

### 4.2 Tracking over long time periods, reveals capillaries

Fig. 4 shows the expected velocity profiles recovered for each ULM track, as well as their locations for a MSE-SVD vs LE-SVD. As expected, full tracks contain velocity profiles that decrease then increase in a U-shape (Fig. 4 left). Additionally, we can recover tracks that either start or end fast, indicating the entrances and exits of capillary tracks. Out of a total of 418, 3959, and 7559 tracks in SE-SVD, MSE-SVD, and LE-SVD conditions, respectively, we see that datasets that record for 6 seconds have more entire capillary tracks than short ensemble acquisitions. Moreover, the length of tracks in LE-SVD are longer than both SE and MSE conditions (Fig 4. Bottom). We also see that the number of full tracks is similar between MSE and LE conditions but the percentage of starts (Fig. 4 middle) and ends (Fig. 4 right) are larger with longer ensembles (Table 1).

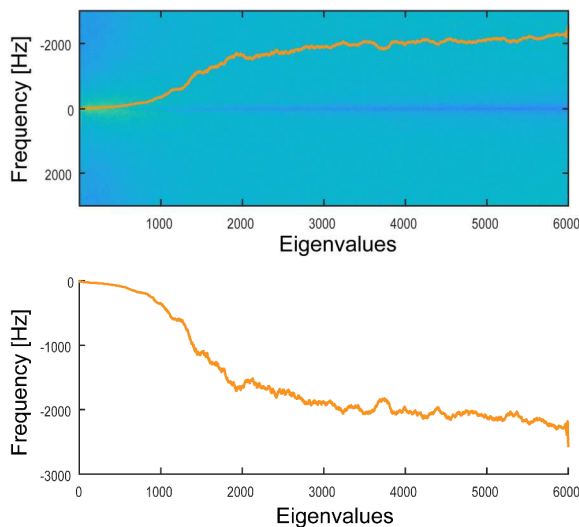


**Fig. 3.** Power spectral density plots for LE-SVD conditions.

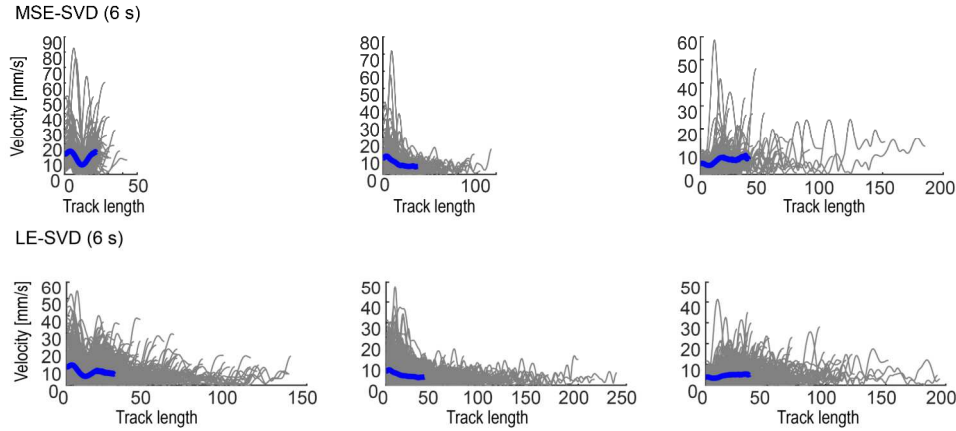


**Fig. 4.** Categorized velocity traces over time. (Top) detected capillaries over complete tracks, entrances, and exits for MSE-SVD. (Bottom) LE-SVD. The blue lines represent the mean illustrating expected velocity profiles.

	SE-SVD (0.6 s)	MSE-SVD (6 s)	LE-SVD (6 s)
<b>Full (%)</b>	0.72	5.13	4.57
<b>starts (%)</b>	0.00	4.59	10.28
<b>ends (%)</b>	0.47	3.46	7.25

**Table 1.** Capillaries as a percentage of all tracks.

### 3. CONCLUSIONS

Long ensemble acquisition SVD clutter filtering changes the overall spectral density, allowing for better discrimination between tissue and recovery of capillary tracks. The main drawback of such a technique is the increased costs in terms of memory availability as well as the computational time. Evidently, this study shows that the number of capillary tracks using short ensembles is very low. Even if large datasets are taken, if they are not continuous, then most capillary tracks remain unrecoverable. Here, LE-SVD clutter filtering recovers more capillary tracks per dataset. Future investigations involve further exploration of using dynamic classification for biomarker discovery and potential coupling with backscattering amplitude methodologies.

### 4. ACKNOWLEDGEMENTS

This work is supported by the Vanier-Banting Postdoctoral Fellowship administered by NSERC, TransMedTech Institute Living Lab postdoctoral scholarship, and the Canadian Institutes of Health Research (CIHR) under Grant 452530.

### 5. REFERENCES

[1] O. Couture, V. Hingot, B. Heiles, P. Muleki-Seya, and M. Tanter, "Ultrasound localization microscopy and super-resolution: A state of the art," *IEEE Trans. Ultrason. Ferroelectr. Freq. Control*, vol. 65, no. 8, pp. 1304–1320, Aug. 2018.

[2] C. Demené *et al.*, "Spatiotemporal Clutter Filtering of Ultrafast Ultrasound Data Highly Increases Doppler and fUltrasound Sensitivity," *IEEE Trans. Med. Imaging*, vol. 34, no. 11, pp. 2271–2285, Nov. 2015.

[3] C. Bourquin, J. Poree, F. Lesage, and J. Provost, "In Vivo Pulsatility Measurement of Cerebral Microcirculation in Rodents Using Dynamic Ultrasound Localization Microscopy," *IEEE Trans. Med. Imaging*, vol. 41, no. 4, pp. 782–792, Apr. 2022.

[4] Ş. E. Erdener *et al.*, "Dynamic capillary stalls in reperfused ischemic penumbra contribute to injury: A hyperacute role for neutrophils in persistent traffic jams," *J. Cereb. Blood Flow Metab.*, vol. 41, no. 2, pp. 236–252, Feb. 2021.

[5] Ş. E. Erdener and T. Dalkara, "Small vessels are a big problem in neurodegeneration and neuroprotection," *Front. Neurol.*, vol. 10, no. AUG, p. 471685, Aug. 2019.

[6] J. Foiret, H. Zhang, T. Ilovitsh, L. Mahakian, S. Tam, and K. W. Ferrara, "Ultrasound localization microscopy to image and assess microvasculature in a rat kidney," *Sci. Reports* 2017 71, vol. 7, no. 1, pp. 1–12, Oct. 2017.

[7] A. Leconte *et al.*, "A Tracking prior to Localization workflow for Ultrasound Localization Microscopy," Aug. 2023.

[8] B. Heiles, A. Chavignon, V. Hingot, P. Lopez, E. Teston, and O. Couture, "Performance benchmarking of microbubble-localization algorithms for ultrasound localization microscopy," *Nat. Biomed. Eng.* 2021 65, vol. 6, no. 5, pp. 605–616, Feb. 2022.

[9] A. Linninger, G. Hartung, S. Badr, and R. Morley, "Mathematical synthesis of the cortical circulation for the whole mouse brain-part I. theory and image integration," *Comput. Biol. Med.*, vol. 110, pp. 265–275, Jul. 2019.